Energy Reports 6 (2020) 672–683

Contents lists available at ScienceDirect

Energy Reports

journal homepage: www.elsevier.com/locate/egyr

Research paper

A rapid classification method of the retired $LiCo_xNi_yMn_{1-x-y}O_2$ batteries for electric vehicles

Ping Zhou [a], Zhonglin He [a], Tingting Han [b], Xiangjun Li [c], Xin Lai [a], Liqin Yan [b], Tiaolin Lv [b], Jingying Xie [b], Yuejiu Zheng [a,*]

[a] College of Mechanical Engineering, University of Shanghai for Science and Technology, Shanghai 200093, PR China
[b] Shanghai Institute of Space Power-Sources, Shanghai 200245, PR China
[c] Electrical Engineering and New Material Department, China Electric Power Research Institute, Beijing 100192, PR China

ARTICLE INFO

Article history:
Received 17 December 2019
Received in revised form 2 March 2020
Accepted 11 March 2020
Available online xxxx

Keywords:
Retired lithium-ion battery
Rapid classification
Capacity estimation
Battery pack
RBFNN

ABSTRACT

With the aging of Lithium-ion batteries (LIBs) of electric vehicles in the near future, research on the second use of retired LIBs is becoming more and more critical. The classification method of the retired LIBs is challenging before the second use due to large cell variations. This paper proposes a rapid classification method based on battery capacity and internal resistance, because batteries with different capacities and internal resistances have different voltage curves during charge/discharge. First, the piecewise linear fitting method established by the specified tested batteries with capacities and their corresponding characteristic voltages is used to sort the batteries. Then combined with the nonlinear function approximation ability of the radial basis function neural network (RBFNN) model, battery capacity and internal resistance are predicted after the model training. 108 cells are used for the simulation classification with experimental classification performed on 12 cells. The results prove that the classification method is accurate.

1. Introduction

With the rapid development of new energy vehicles, a big problem about how to dispose the large amounts of retired batteries occurs. Currently, there are two ways to dispose the retired Lithium-ion batteries (LIBs) —directly recycled or recycled after second use. The fields of second use of retired LIBs include low-speed electric vehicles(EVs), mobile power, energy storage for family use and so on. Since 70%–80% of the capacity of retired battery can be used, the second use of the retired LIBs could be attractive.

An early approach to the topic of the retired battery second use was conducted by the U.S. Advanced Battery Alliance (USABC), in which Pinsky et al. studied the technical and economic feasibility of using a secondary Nickel Metal Hydride (NiMH) EV batteries (Pinsky et al., 2002). Saxen et al. discussed the applicability that the retired battery standard capacity is 80% of the initial battery so that the battery can meet the customer's EV capability during aging (Saxena et al., 2015). On the economic aspect, research has shown that it is profitable to use retired lithium batteries for backup power and energy storage sites (Assunção et al., 2016a,b; Heymans et al., 2014; Ahmadi et al., 2014a; Gur et al., 2018; Xu et al., 2019). Gur et al. conducted a comprehensive review of existing waste battery projects and considered that appropriate fiscal incentives were needed to encourage investment in such systems (Gur et al., 2018). Neubauer et al. studied the impact of secondary battery use on customers based on the initial cost of EV batteries and explored the potential of second-hand EV batteries in the grid energy storage application market. It has been found that it is likely to become a common part of the life cycle of automotive batteries in the future and may transform markets in need of cost-effective energy storage (Neubauer and Pesaran, 2011). Tong et al. studied the feasibility of installing a second-stage battery pack in a off-grid photovoltaic vehicle charging system, and considered that a system using a second-life battery system could achieve similar performance to a new battery system, but at a reduced cost (Tong et al., 2013). Jiao et al. believed that the secondary use of retired batteries could potentially promote business model innovation and link the current isolated transportation field to the energy applications (Jiao and Evans, 2016). Linda Gaines described a working system that used the lead–acid battery recycling as a recycling model with considerations what steps could be taken to avoid recycling barriers and ensure an economical and sustainable choice at the end of battery life (Gaines, 2014). Ambrose et al. simulated the resource and potential performance of retired batteries in rural areas, as well as technical and economic aspects, and concluded that a large number of retired vehicle batteries can provide electricity to

* Corresponding author.
E-mail address: yuejiu.zheng@usst.edu.cn (Y. Zheng).

https://doi.org/10.1016/j.egyr.2020.03.013

rural users (Ambrose et al., 2014). Ziyou Song et al. investigated and compared the profits that second-life and fresh batteries can bring to wind farm owners. And they believed second-life batteries might outperform fresh batteries in the future if the wind energy price could decreases faster than the battery price (Song et al., 2019). Lluc Canals Casals et al. studied a technical and economic analysis of the secondary electricity markets in Europe and the monitoring data of a second-life EV battery that installed in a library in Montgat, Barcelona, Spain. This study showed that battery lifespan increases by a 35% with the incorporation of second life applications in buildings. Moreover, second-life batteries could reduce the effective price of EVs and reduce its life cycle impacts (Casals et al., 2019). Silvia Bobba et al. developed a dynamic stock and flows model to describe the life-cycle steps and processes along the value-chain of lithium batteries after their removal from electric vehicles in Europe. They believed this study contributed to a more-in depth knowledge of the second-use of batteries and its potential effects in Europe (Bobba et al., 2019). In terms of the environment, the second use of retired batteries from EVs can greatly reduce carbon dioxide emissions and improve air quality (Martinez-Laserna et al., 2018; Sathre et al., 2015; Ahmadi et al., 2014b).

A battery pack in an EV is composed of dozens or even hundreds of single battery cells connected in series and in parallel, thereby obtaining high voltage and high capacity. However, battery cells in the same batch made by the same manufacturer will be inconsistent more or less. Besides, during the stage of the EV usage, battery cells decay at varied speeds when the environment is different (especially when temperatures are different). Therefore, battery cells will be more different from each other after the EV usage. It is very important to achieve accurate predictions of the remaining battery life and battery state under various operating conditions (Hu et al., 2020, 2019, 2018; Zheng et al., 2019; Zhang et al., 2019; Tian et al., 2019). This is essential for the battery management system to ensure reliable operation and timely maintenance and is also critical for battery second-life applications.

According to relevant documents, the inconsistency of retired lithium batteries for reuse will be more severe than original ones (Dubarry and Liaw, 2009; Barré et al., 2013; Paul et al., 2013; Zheng et al., 2015; Baumhöfer et al., 2014; Schuster et al., 2015). Problems such as over-charge and over-discharge, or even thermal runaway accidents are more likely to happen. Therefore, before the second use, the retired lithium batteries shall be classified. Batteries with the same features shall be picked out to construct new battery packs in series and parallel with less difference. Baumhöfer et al. experimented with 48 cells from a large-scale production line, using data mining algorithms to identify the dependence between initial battery performance and cycle life, resulting in a linear regression model that predicts lifetime, and believe it can be used to classify batteries into different batches before battery pack production (Baumhöfer et al., 2014). The method can estimate battery performance good, but this method requires extensive tests of multiple stages to determine the current battery performance. The process may also be affected by many factors. Kaizheng Fang et al. realized that the battery was divided into different heating categories by collecting the heat data generated by the nickel-metal hydride battery during charging (Fang et al., 2013). In this method, thermal behaviors are used for classification, but however, the heat data are also hard to be quickly achieved. Chengbao Liu et al. used a convolutional neural network (CNN) for LIBs screening, and the results showed that lithium battery inconsistency can be greatly reduced (Liu et al., 2018). This method uses deep learning method which is suitable for battery classification. Nevertheless, it first needs to test the battery capacity, then classify the batteries according their capacity. At last, the classified battery needs to be discharged completely, and thus is very labor intensive. Liao et al. (2017) and Li et al. (2017) conducted a classification of retired LIBs by observing the appearance of the battery, battery capacity measurement, pulse characteristic curve and electrochemical impedance spectroscopy. Their approaches are good to achieve a comprehensive judgment and accurate classification, but they require a variety of different performance tests and thus are time consuming. Our research group proposed a capacity estimation method based on charging voltage curves. In the demonstration of the basic theory, the capacities of other series-connected batteries in the battery pack are estimated by the method of shifting and scaling the charging curve to make the charging voltage curve of other cells coincide with the charging voltage curve of a known capacity of the battery pack, which can be used to classify batteries of different capacities (Zheng et al., 2013). For traditional classification, each retired lithium battery shall be fully charged and discharged, by which the internal resistance, capacity, self-discharge and other parameters can be achieved; after that, the retired batteries with the same parameters will be selected and formed in series–parallel to form new battery packs. In fact, it costs a lot, both time and money. Therefore, it is not applicable for disposing large amounts of retired lithium batteries. Recently, via parallel equalization of the retired batteries, followed by short-term fast series charging, we classified the batteries of different capacities according to the inherent relationship between charging voltage changes and capacity (Lai et al., 2019). However, the parallel equalization process cannot be applied for battery modules. Nevertheless, in real applications, batteries before reuse are usually hard to be disconnected as the modules are usually connected by welding. Under this background, we (Lai et al., 2018) further proposed a fast discharge classification method in which each cell had a short-term series discharge after they were fully charged, and then model training and capacity computing were carried out by genetic algorithm back propagation (GA-BP). Unfortunately, because of the single input single output (SISO) of this method, it is not so good for classifying both the capacity and internal resistance.

In this paper, short-term series discharge after being separately fully charged of each cell are used to exam the battery characteristics; furthermore, radial basis function neural network (RBFNN) model is established with the multi-dimensional input of characteristic voltages and multi-dimensional output of the internal resistance and capacity. In this way, batteries can be classified fast while the classification accuracy regarding the internal resistance and capacity can be highly guaranteed. With the basic principle of the battery classification for the capacity and internal resistance, two classification methods—the piecewise linear fitting (PLF) method and the RBFNN method are put forward, which can be used to classify retired lithium batteries in different amounts. The PLF model is established by some tested batteries with capacities and their corresponding characteristic voltages. Capacities of the remaining batteries can be obtained by substituting characteristic voltages into the model. But the PLF method requires organized data of the tested batteries, and may not be suitable for large-scale battery classification. The RBFNN method randomly selects some retired batteries for model training, and then uses this model to predict the internal resistance and capacity of the rest retired batteries. When it comes to classify large-scale batteries, these two methods can be used in combination. Firstly, the PLF method is used to collect a batch of data. Then the data is used for the RBFNN method for training, which achieves the transition from small-scale to large-scale battery classification.

The structure of this paper is as follows: Section 2 describes the principle and the methods of classification. Simulations and

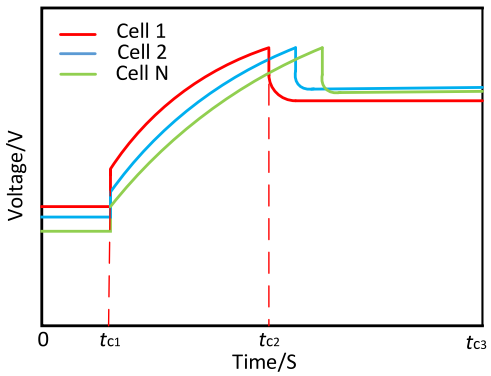

Fig. 1. Cell charging voltage curves.

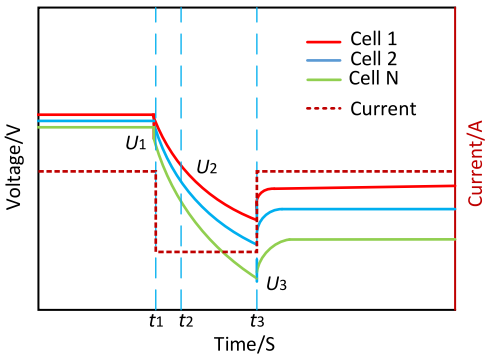

Fig. 2. Module discharging voltage curves.

experiments are described in Section 3. In Section 4, simulation and experimental results are analyzed with proposed methods. Section 5 discusses the evaluation of classifying results, advantages and disadvantages of methods, and the economics. Section 6 gives a summary of the paper.

2. Classification principle and methods

2.1. Classification principle

For retired lithium batteries of the same type, internal resistances and capacities are quite different. The same charge rate is used for each cell in the modules until an identical voltage is reached, and then the voltage drops after the cell is stored for some time. It is known that polarization and diffusion processes are observed in lithium batteries, which are generally considered as the internal resistances. The higher internal resistance is, the higher voltage drop will be and vice versa. Batteries with different internal resistances can be classified according to this simple characteristic. If batteries with the same initial voltage and internal resistance are discharged in series for a period of time, batteries with different capacities will have different discharge curves. The higher capacity is, the lower voltage drop will be and vice versa. So batteries with different capacities can be classified if the effects of the internal resistance difference are firstly eliminated.

Based on the aforementioned principle, this paper describes the following classification process. First, retired LIBs in the same batch will be charged independently, whose charge rate and cut-off voltage are set the same. Fig. 1 shows the schematic diagram of the cell charging voltage curves. Cell 1 is under rest from the time 0 to t_{c1}; it is charged from time t_{c1}, and stopped at t_{c2} when it reaches charge cut-off voltage. A voltage relaxation process is observed after t_{c2}. After voltage relaxation process, the open circuit voltages (OCV) of all cells are sorted in an ascending order and cells with the OCV difference within 0.002 V are divided into one group, which means cells with similar internal resistance are classified into one group.

Fig. 2 shows the schematic diagram of the discharge curves of the modules. t_1 is the time to start discharging and the voltage at this time is U_1;t_2 is the time after 10 s discharge, and the voltage at this time is U_2;t_3 is the time after 5 min discharge and the voltage at this time is U_3. During t_1 to t_3, the change of the cell voltage consists of two parts. One is caused by the polarization of the cell, it is U_R which is equal to the voltage difference during t_1 to t_2, as is shown in formula (1). Because the time of discharge from t_1 to t_2 is too short, it can be considered that the amount of electricity discharged during this period has no effect on the OCV of the cell, so the voltage change in this part is considered to be caused by the internal resistance. The other part is the drop of the OCV, which is caused by the state of charge (SOC) change during the discharge. This part is marked as U_d as is shown in formula (2). U_d excludes the interference of the 10 s internal resistance voltage, and can be attributed largely to the amount of electricity discharged. Because the SOC drops are different due to the different capacities of battery cells, we can see that U_d of the cells in the modules are different. Therefore, U_d can be used for the capacity classification.

$$U_R = U_1 - U_2 \tag{1}$$

where U_R is the 10 s internal resistance voltage of the cell, U_1 is the initial voltage before discharge, and U_2 is the voltage after 10 s discharge.

$$U_d = U_2 - U_3 \tag{2}$$

where U_d is the OCV drop caused by discharge, and U_3 is the voltage after 5 min discharge.

2.2. Classification method

2.2.1. Piecewise linear fitting method

By formula (2), U_d of battery cell in each group can be obtained. Taking a certain group as an example, U_d of battery cells are sorted in an ascending order, that is $[U_{d\,\min} \ldots U_{d\,\max}]$. According to the voltage difference $(U_{d\,\max} - U_{d\,\min})$ and quantity of cells, the cells are properly n-partitioned, then the ith section is $[U_{d\,\min} + (i-1)(U_{d\,\max} - U_{d\,\min})/n,\ U_{d\,\min} + i(U_{d\,\max} - U_{d\,\min})/n]$. For each section, the isometric sampling is done as shown in Fig. 3. Three cells are sampled in the ith section and subjected to standard capacity test. Since it is not guaranteed that the U_d of the sample cell corresponds to the sample voltage U in each section, it can be replaced by the cell which is the closest to the sample voltage U. After U_d and capacity C of the three sample cells are obtained, linear fitting can be performed, and the fitting parameters k and f of the ith section will be obtained, as shown in formula (3). The capacities C of the remaining cells in the ith section can be obtained by substituting U_d into formula (3). By performing the same process in other sections, the fitting parameters k and f of all sections can be obtained. Thereby the capacity of all sections can be obtained. Finally, other groups can be performed in the same way and the capacity of each cell can be obtained.

$$C = k \times U_d + f \tag{3}$$

where C is the battery capacity, k and f are the fitting parameters.

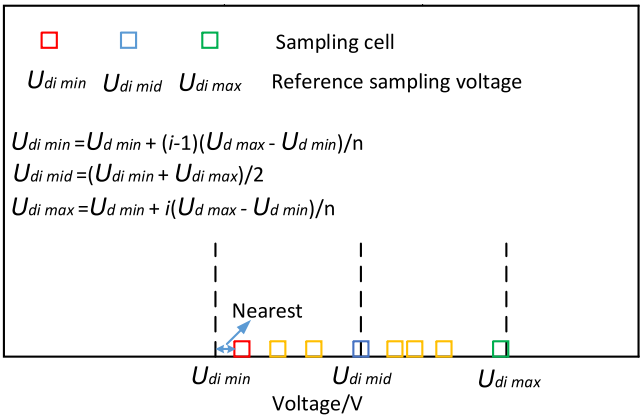

Fig. 3. Isometric sampling for Section i.

2.2.2. Radial basis function neural network method

For the method mentioned above, it is mandatory to sort and group the batteries. If there are large amounts of retired batteries, the classification would be quite complicated and would not be so efficient. Thus, the RBFNN method is put forward. Relying on nonlinear mapping function owned by RBFNN input and output, model training is performed on some already-know data, and then use the already-trained model to predict the new data.

The artificial neural network is modeled and linked based on the basic unit of human brain — neuron, simulating the human brain nervous system, forming an artificial system with intelligent information processing such as learning, association, memory and pattern recognition. RBFNN can use a supervised learning algorithm to obtain the weight parameters of the neural network through training sample data, so that the error between the final output result and the actual result is minimized. Since RBFNN essentially implements the mapping function from input to output, and mathematical theory proves that it has the function of realizing any complex nonlinear mapping, it can be used to solve complex internal mechanisms, making it suitable for regression prediction, classification and recognition and other issues. Therefore, this paper uses the RBFNN model to conduct training on battery data, such as characteristic voltages, internal resistances and capacities. After that, the model can be used to predict the internal resistance and capacity of other batteries. RBFNN consists of input layer, hidden layer and output layer. The flow chart is shown in Fig. 4.

For the RBFNN model in this paper, it is mandatory to train some battery data first. The input are the characteristic voltage U_1, U_2 and U_3 collected during the series discharge, and the output are capacity C and internal resistance R, where the internal resistance R can be obtained by formula (4) and the capacity is achieved by the full charge and discharge experiments. Before the training, the data needs to be normalized. The specific method is to change the number to a decimal between $(-1, 1)$, such as formula (5), which make it easier to process data, speed up the convergence of network training and improve training speed. When the training is completed, input a new group characteristic voltage U_1, U_2 and U_3, then the capacity C and the internal resistance R can be estimated. The estimation process is indicated by the blue arrow in Fig. 4.

$$R = U_R / I_{dsc} \tag{4}$$

where R is the internal resistance of the battery, I_{dsc} is the discharge current.

$$X = 2(U - U_{min})/(U_{max} - U_{min}) - 1 \tag{5}$$

where $U_{\max}$ and $U_{\min}$ are the maximum and minimum values of the voltage U in the samples.

3. Simulation and experiment

3.1. Simulation

The simulation uses a second-order resistor-capacity(RC) equivalent circuit model, which includes an ideal electromotive force E, a pure ohmic internal resistance R_0 and two polarized RC parallel circuits, as is shown in Fig. 5. R_1, R_2 are polarized resistors, and C_1, C_2 are polarized capacitors. The parallel circuit composed by R_1 and C_1 represents the polarization of the electrode, and the parallel circuit composed by R_2 and C_2 represents the concentration polarization. The model can not only correctly test the parameters, whose computing error is quite small; but also it can well reflect the dynamic and static feature of the battery. The model formula is shown in (6).

$$U_L = E - I_L R_0 - U_1 - U_2 \tag{6}$$

where U_L is the terminal voltage of the cell, E is the electromotive force, I_L the current, R_0 the ohmic internal resistance, U_1, U_2 the terminal voltages of the two RC circuits respectively.

The single cell model also includes a thermal model. Because temperature has a large impact on cell performance, the thermal model is the basis for other submodels. In addition, other submodels are included, including SOC calculation model, voltage model, internal resistance model, aging model, Coulomb efficiency model, capacity decay model, self-discharge model and so on. Finally, a battery pack system model is build which contains 108 single cells, as is shown in Fig. 6. This battery pack system model includes a battery pack, information output, and power system. The battery pack consists of 108 single cells connected in series. The information output function mainly records and exports data for analysis. The main function of the power system is to control the charge and discharge of the battery. One may refer to our preliminary work (Zheng et al., 2014) for more information about the battery pack system model.

The simulation process is shown in Fig. 7. (1) Firstly, 108 battery capacities are randomly set. In order to make the simulation more in line with the actual situation, the setting of battery capacity refers to the batteries used in real applications. When setting battery capacity, the real battery original capacity (60%–90%) is used as the selection range and obtained by using MATLAB unifrnd function. Since the unifrnd is a continuous uniform random function, we can see a uniform distribution in the figure. (2) The 108 battery cells are individually charged with the same charging rate($1/3C_{rate}$, and C-rate is the measurement of the charge and discharge current with respect to its nominal capacity, and a fully-charge battery is fully discharged in 3 h with 1/3C-rate current), and the charging cut-off voltage is 4.15 V. After charging, the battery cells are rest for relaxation to achieve OCVs. (3) all the battery cells are discharged in series with 5 min, and the discharge rate is $1C_{rate}$. Finally, according to the classification principle and method mentioned in Section 2, the capacities and internal resistances of the cells will be estimated.

3.2. Experiment

A total of 12 $LiCo_xNi_yMn_{1-x-y}O_2$(NCM) cells of different ages were selected in this experiment. The basic parameters are shown in Table 1.

The experimental procedure is shown in Fig. 7.

(1) Standard capacity test on the selected 12 cells are firstly carried out. Because results of each test are slightly different, capacities will be calculated for three times and the average will be taken as the standard capacity for corresponding cells.

(2) The 12 cells are charged separately with $1/3C_{rate}$, and the charging cut-off voltage is 4.15 V. After charging, the cells will be rest for 3 h to achieve the OCV.

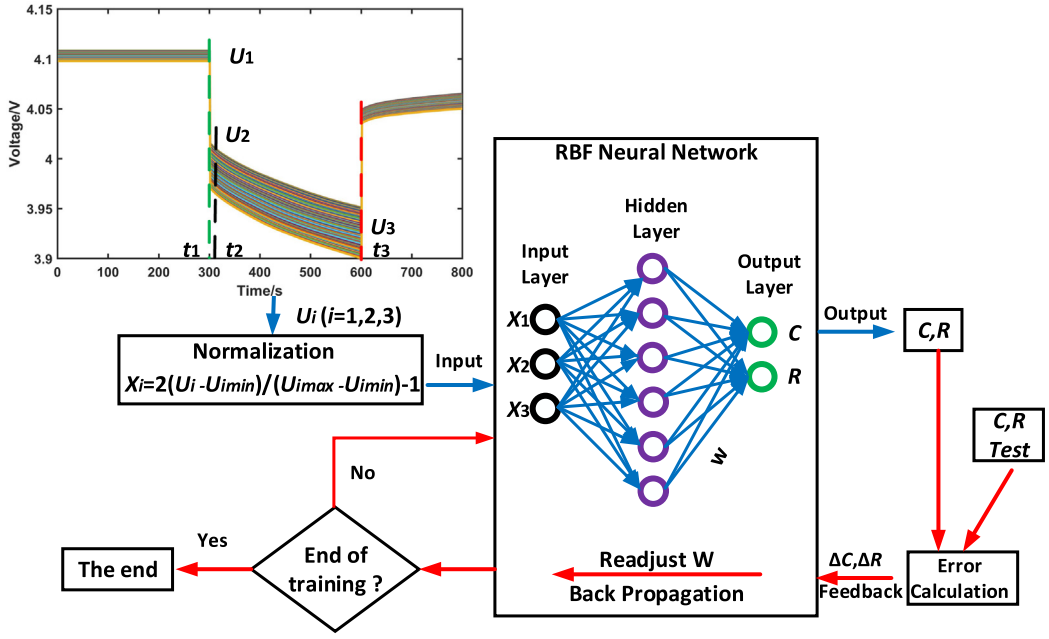

Fig. 4. Flow chart of the RBFNN method . (For interpretation of the references to color in this figure legend, the reader is referred to the web version of this article.)

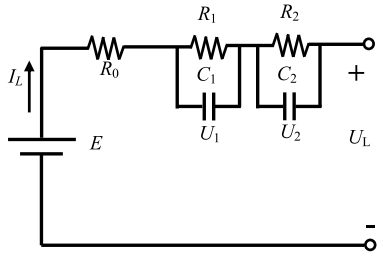

Fig. 5. Second-order RC model.

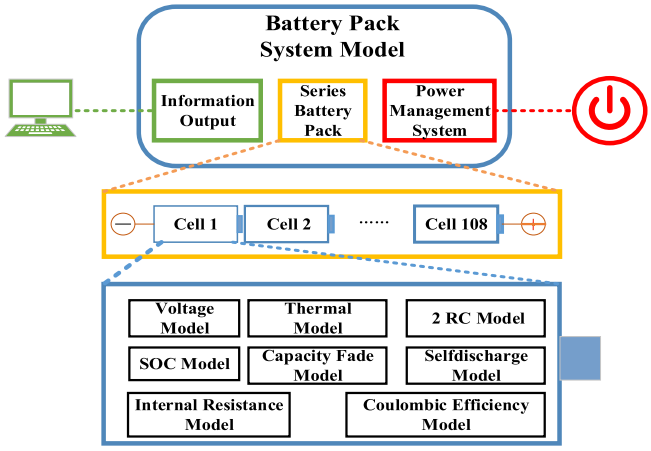

Fig. 6. Battery pack system model.

(3) 12 cells in series are discharged with $1C_{rate}$, and the discharge lasts 5 min. According to the classification principle and method in Section 2, capacities and internal resistances of the cells will be estimated.

Table 1
Basic parameters of NCM battery.

Item	Specification	Item	Specification
Nominal capacity	32.5 Ah	Standard charge current	11 A ($1/3C_{rate}$)
Nominal voltage	3.75 V	Standard discharge current	11 A ($1/3C_{rate}$)
Maximum charge current	65 A ($2C_{rate}$)	Charge cut-off voltage	4.15 V
Maximum discharge current	65A ($2C_{rate}$)	Discharge cut-off voltage	2.5 V
Storage temperature	−40∼70 °C	Operating temperature	−25∼60 °C

4. Results and analysis

4.1. Simulation and experimental results based on the PLF method

4.1.1. Simulation results based on the PLF method

According to the classification principle and method described in Section 2, the cell characteristic voltages U_1, U_2 and U_3 corresponding to the times t_1, t_2, and t_3 are collected, and the internal resistances of cells can be obtained by formulas (1) and (4), as are shown in Fig. 8. According to the classification principle described in Section 2, U_1 is sorted in an ascending order and cells with the voltage difference within 0.002 V are divided into one group. The general results are shown in Table 2. U_d of each cells are figured out via formula (2). Subsequently, the cells are sorted in an ascending order according to the respective U_d in each group. The number of sections is decided according to the voltage difference ($U_{d\,\max} - U_{d\,\min}$) and the quantity of cells. The results are shown in Table 2.

Group 7 has the largest number of cells, so we take it as an example. According to the voltage difference ($U_{d\,\max} - U_{d\,\min}$) and cell quantity, the cells in Group 7 are divided into 2 sections, as are shown in Table 3. In Section 1, 3 of the 9 cells (Cell 5,74 and 102) are selected to have the capacity test according to the isometric sampling. The fitting parameters $k_{71} = -1052$ Ah/V, $f_{71} = 93.56$ Ah are obtained after linear fitting. In Section 2, 2 of the 4 cells (Cell 45 and 100) are selected to have the capacity

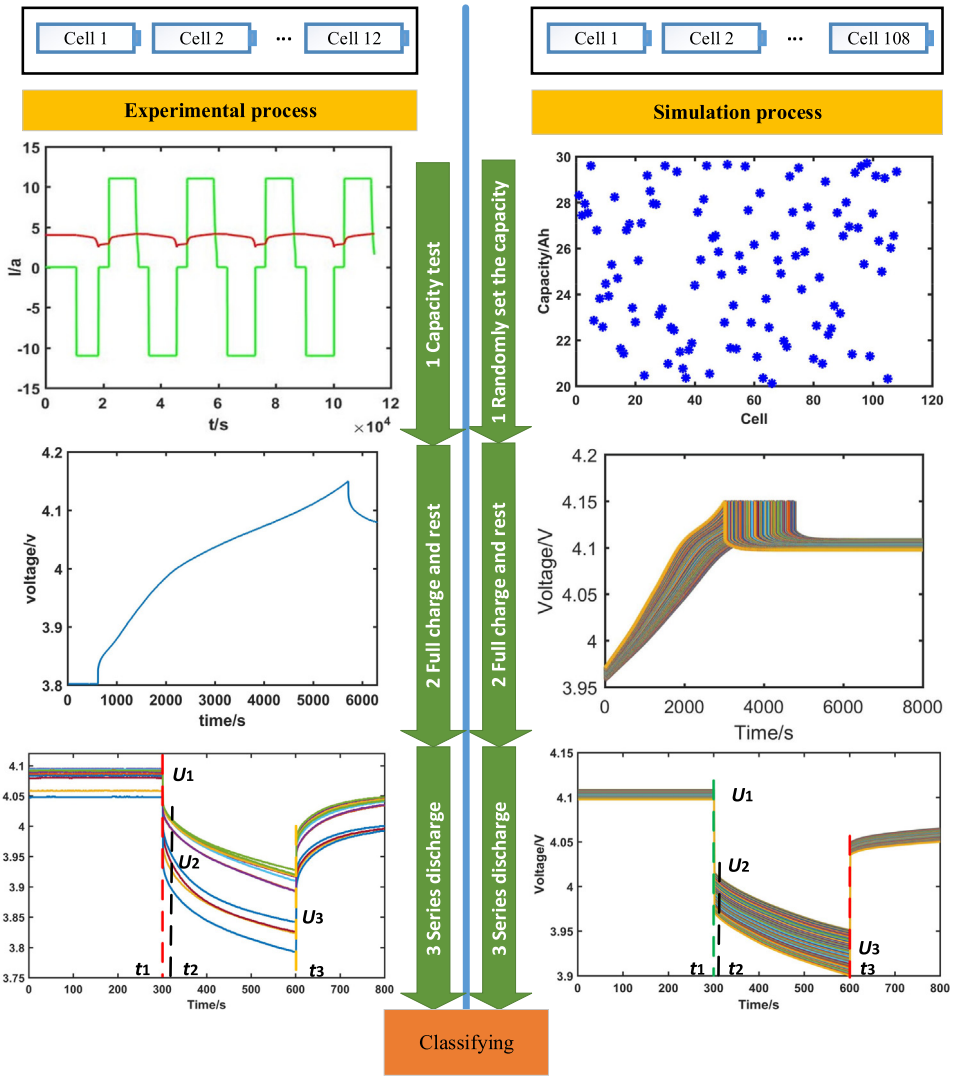

Fig. 7. Simulation and experimental process.

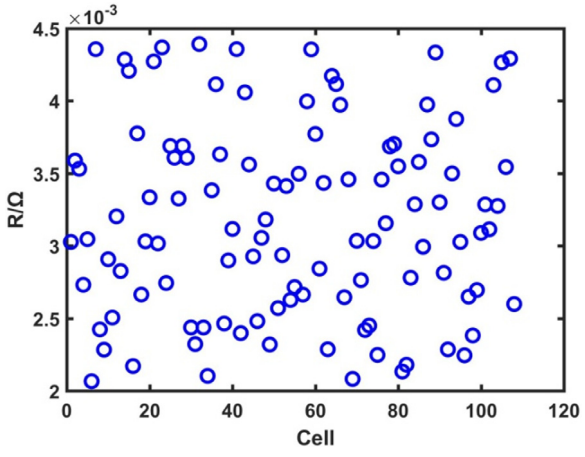

Fig. 8. Internal resistances of the 108 cells in simulation.

test. The fitting parameters $k_{72} = -1104.87$ Ah/V, $f_{72} = 98.4268$ Ah are obtained after linear fitting. According to formula (3), the estimated capacities of cells in each section can be obtained by U_d. The estimation results and errors are shown in Fig. 9 and Table 3.

Table 2
Groups and sections for the 108 cells in simulation.

Group (U_1/V)	Number of cells	Number of sections (n)
Group 1 (4.0973∼4.0993)	11	2
Group 2 (4.0993∼4.1013)	7	1
Group 3 (4.1013∼4.1033)	3	1
Group 4 (4.1033∼4.1053)	12	2
Group 5 (4.1053∼4.1073)	11	2
Group 6 (4.1073∼4.1093)	10	2
Group 7 (4.1093∼4.1113)	13	2
Group 8 (4.1113∼4.1133)	10	1
Group 9 (4.1133∼4.1153)	9	2
Group 10 (4.1153∼4.1173)	11	2
Group 11 (4.1173∼4.1193)	11	2

Similar processes are done for the other groups, and the result is shown in Fig. 10. From the result, we can see that the capacity estimation is quite accurate, and the maximum error does not exceed ±4.2%.

4.1.2. Experimental results based on the PLF method

In the experiment, the cells were firstly tested to achieve the capacities and resistances. The results are shown in Table 4. The

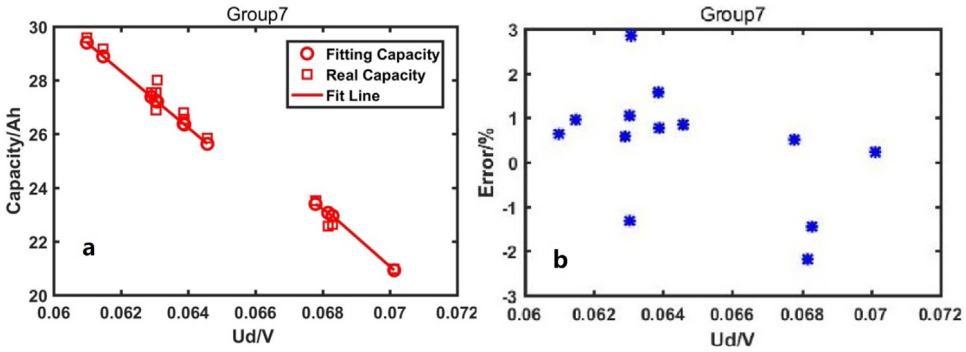

Fig. 9. Estimation capacities and errors in Group 7. (a) Capacity estimation; (b) Capacity estimation errors.

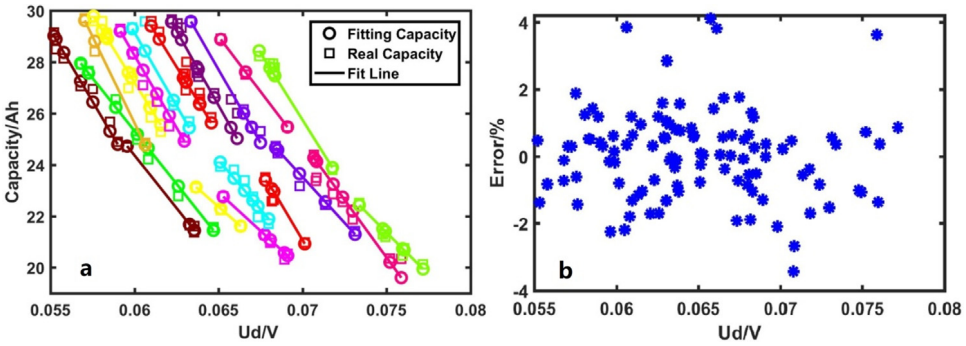

Fig. 10. Estimation results and errors using the PLF method in simulation. (a) Capacity estimation; (b) Capacity estimation errors.

Table 3
Capacity estimation results based on the PLF method for Group 7 in simulation.

	Section 1								
Cell	**5**	95	70	72	**102**	52	86	19	**74**
U_d/V	**0.0610**	0.0615	0.0629	0.0630	**0.0630**	0.0631	0.0639	0.0639	**0.0646**
Real Capacity/Ah	**29.5929**	29.1719	27.5469	27.5373	**26.8921**	28.0028	26.7970	26.5574	**25.8526**
Estimated Capacity/Ah	29.388	28.862	27.3892	27.284	27.284	27.1788	26.3372	26.3372	25.6008
Error/%	0.69	1.06	0.57	0.92	−1.46	2.94	1.72	0.83	0.97

	Section 2			
Cell	**45**	47	1	**100**
U_d/V	**0.0678**	0.0682	0.0683	**0.0701**
Real Capacity/Ah	**23.5166**	22.5751	22.6297	**20.9754**
Estimated Capacity/Ah	23.5166	23.0747	22.9642	20.9754
Error/%	0	−2.21	−1.47	0

Note: The sampled batteries are shown in bold.

Table 4
12 cell capacity, resistance and U_1.

Cell	1	2	3	4	5	6
Capacity/Ah	24.9983	28.2313	24.3978	28.6667	29.8928	28.0153
Resistance/Ω	0.0038	0.0027	0.0039	0.0026	0.0024	0.0026
U_1/V	4.083	4.086	4.058	4.094	4.093	4.094
Cell	7	8	9	10	11	12
Capacity/Ah	25.599	22.646	29.341	29.2559	28.320	28.885
Resistance/Ω	0.0041	0.0046	0.0025	0.0024	0.0028	0.0023
U_1/V	4.08	4.048	4.092	4.09	4.09	4.091

Table 5
Groups for the experiment cells.

	Group 1			Group 2			
Cell	4	5	6	9	10	11	12
U_1/V	4.094	4.093	4.094	4.092	4.09	4.09	4.091
U_2/V	4.017	4.021	4.017	4.018	4.017	4.006	4.021
U_3/V	3.916	3.927	3.909	3.917	3.918	3.892	3.92

different values of U_1 prove that the batteries with different internal resistances have different voltage drops after fully charged and rested that described in Section 2.

The series discharge experiment is performed. The results are shown in Table 5. According to the classification principle described in Section 2, U_1 is sorted in an ascending order. The cells with voltage difference within 0.002 V are grouped into one group, which means cells with similar internal resistance are classified into one group. Because some cells have a large difference in U_1 from others and the quantity is not enough, these cells are not grouped. Since there are not many cells in each group, sections are not required in each group.

Next, the linear fitting is performed. In group 1, Cell 5 and 6 are selected to do the linear fitting according to the sampling principle. The fitting parameters $k_1 = -134.1071$ Ah/V, $f_1 = 42.4989$ Ah are obtained. In group 2, Cell 10 and 11 are selected to do the linear fitting and the fitting parameters are $k_2 = -62.3933$ Ah/V, $f_2 = 35.4328$ Ah. Capacities of each group can be obtained by U_d according to formula (3), and the estimated results and errors are shown in Table 6. The results show that the estimated

capacity obtained by the PLF is accurate, and the errors are within ±1%.

4.2. Simulation and experimental results based on the RBFNN method

4.2.1. Simulation results based on the RBFNN method

This paper selects the first 50% of 108 cells as training samples, in which U_1, U_2 and U_3 are used as the input training data, and the capacity C and internal resistance R are used as the output training data. After the training is completed, the remaining 50% cells are used as verification samples. Namely, after U_1, U_2 and U_3 are inputted into the RBFNN model, the capacity C and internal resistance R of cells can be estimated. The result is shown in Fig. 11. From the results of Figures b and d, we can see that the prediction of RBFNN is accurate. The maximum error of the capacity does not exceed ±5%, and the maximum error of internal resistance does not exceed ±0.4%, indicating that the RBFNN method can be used to classify large-scale retired batteries.

4.2.2. Experimental results based on the RBFNN method

Since there are only 12 cells in this experiment, the first 8 cells are selected from the 12 cells as the RBFNN training samples, and the remaining 4 cells are used for verification. The results are shown in Fig. 12. From Figures b and d, we can find that the maximum error of the capacity does not exceed ± 5%, and the maximum error of internal resistance does not exceed ± 1%. Though the experimental data is not many, the estimation accuracy of the RBFNN model is still reliable.

5. Discussion

Two methods proposed in this paper can be used for accurate estimation of battery capacity and internal resistance, and further used for battery classification. On this basis, this section further discusses three issues: the first is how to classify the batteries with the estimated capacities and internal resistances and how to evaluate the battery packs after classification; the second is the advantages and disadvantages of above two methods and their respective applicable situations; the third is about the economic analysis of the methods proposed in this paper comparing with traditional methods.

5.1. Evaluation of the classification

The basic idea of the classification evaluation is simple and direct: the batteries are regrouped according the capacities and internal resistances, and experimented in a certain test condition to see whether the voltage difference is smaller than an arbitrary regroup. In this paper, two groups of single cells are selected from simulation cells and experimental cells respectively and connected in series into two battery packs, and then the discharge test is performed. The voltage difference between the two battery packs is observed from the discharge curve.

5.1.1. Simulation classification

In group 5 Section 2, we select cell 3, cell 62, cell 68, cell 93 and cell 35 to form a battery pack in series, which is named Pack A. We also randomly select 5 cells from the 108 cells, whose numbers are 1, 25, 52, 73 and 100, and connect them in series into a battery pack, which is named Pack B. The discharge test is performed on the two battery packs using $1/3C_{rate}$, and the discharge last 1 h. The results are shown in Fig. 13. The voltage consistency of the discharge curve of Pack A is better. At the end of discharge, the cell voltage difference of Pack A is 0.0195 V; the cell voltage difference of pack B is 0.0553 V. The root mean square error (RMSE) of the discharge curves of the two battery packs are calculated. The RMSE in Pack A is 0.004 V, and the RMSE in Pack B is 0.01208 V. It is obviously that the batteries classified have good consistency.

5.1.2. Experimental classification

In the above experiment, we have classified out two groups of cells with similar capacity and internal resistance from 12 cells as shown in Table 6. One group containing 4 cells (Cell 9, 10, 11, and 12) are selected and connected in series to form a battery pack, which is named Pack C. Four cells are randomly selected from the 12 cells (Cell 1, 3, 4, and 11) and connected in series to form a battery pack named Pack D. The discharge test is performed on the two battery packs using $1/3C_{rate}$ and last 1 h. The results are shown in Fig. 14. The cell voltage consistency of the discharge curves of Pack C is good. At the end of discharge, the cell voltage difference is 0.004 V, and the RMSE of the discharge curves is 0.002675 V. The discharge curves are scattered and the consistency is poor for Pack D. At the end of discharge, the cell voltage difference is 0.0341 V, and the RMSE of the discharge curves is 0.015525 V. The results demonstrate that the cells classified by the method of this paper have good consistency.

5.2. Applicability of the proposed methods

Simulation and experimental results show that both PLF and RBFNN methods can achieve the classification of retired batteries, but both methods have disadvantages. The PLF is not suitable for large-scale batteries; although the RBFNN method is suitable for large-scale batteries, it requires a batch of known data to perform model training first. Therefore, when faced with large-scale retired batteries, these two methods should used with combination. The first method is used to collect a batch of data, and then the data is used for the RBFNN training to achieving the transition from the small-scale battery classification to the large-scale battery classification. For a better understanding, a further explanation is displayed. When less than a dozen of batteries are required to be classified, which is not the typical case of large scale retired battery classification, we can use the traditional method to perform the full-charge/discharge test on each battery to obtain the capacities and internal resistances, and subsequently classify them according to the achieved results. The traditional method would be time-consuming and power-consuming when the battery scale enlarges to hundreds. The PLF method is then suitable for this scale, with some batteries tested with the traditional method, the PLF method can be easily established. It is not practical to deal with thousands of batteries with the PLF method as some of the cells need to be selected and tested with the traditional method. But we can build a database based of the PLF method which contains dozens of the cell capacities from the PLF method and used to train the RBFNN model. And as a result, the training data of the RBFNN model is no longer a time-consuming process.

5.3. Economic analysis

The traditional method uses fully charge and discharge to achieve battery capacity. The battery generally stores certain power when it leaves the EVs, because the lithium battery itself has a self-discharge phenomenon. If the battery is in an empty state, the self-discharge will cause the battery to be over-discharged which will cause the active material to be lost, thereby reducing the capacity of the battery. If the lithium-ion battery capacity is about 50% when it leaves the EVs, the traditional battery capacity test process is: full charge - full discharge - charge to 50% SOC. The battery test procedure in this paper is: full

Table 6
Estimation results and errors of 2 group cells.

	Group 1			Group 2			
Cell	**5**	4	**6**	**10**	9	12	**11**
U_d/V	**0.094**	0.101	**0.108**	**0.099**	0.101	0.101	**0.114**
Real Capacity/Ah	**29.8928**	28.6667	**28.0153**	**29.2559**	29.341	28.885	**28.320**
Fitting Capacity/Ah	29.8928	28.9541	28.0153	29.2559	29.1311	29.1311	28.320
Error/%	0	−1	0	0	0.72	−0.85	0

Note: The sampled cells are shown in bold.

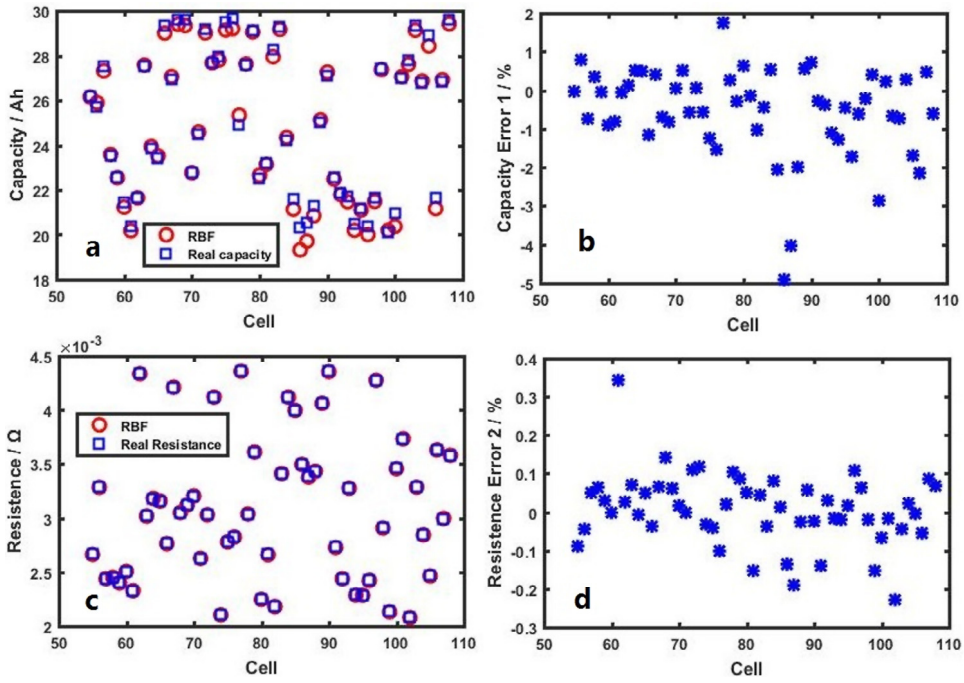

Fig. 11. Estimation results and errors based on the RBFNN method with the simulation data. (a) Capacity estimation; (b) Capacity estimation errors; (c) Resistance estimation; (d) Resistance estimation errors.

charge - series discharge for 5 min. Taking a 110 Wh NCM battery as an example, the energy consumed by full charge is about 120 Wh, and the energy consumed by full discharge is about 118 Wh. Assuming that the average SOC of the retired batteries is 50%, the energy consumed by traditional method is about 238 Wh, while the energy consumed by the method of this paper is only 70 Wh. The power will be reduced to 30% by the methods of this paper. When faced with large-scale retired batteries, the equipment cost saved is very considerable. In terms of the time consumption, the first step of the traditional method and the method in this paper are the same. Although it needs rest for a certain period of time after full charge for the proposed method, but the rest time does not occupy the equipment. So the first step of the both methods take the same equipment time. The proposed method needs to discharge all the batteries in series for 5 min with 1 C_{rate}. Even if the traditional method is calculated according to the fastest time, using $1C_{rate}$ to full discharge in series and then charge in series to 50% SOC, it will take 90 min. It can be concluded that: although the capacity accuracy of the traditional method is 100%, it costs a lot, both equipment and time. The classification method in this paper is not as accurate as the traditional method, but the equipment and time cost is greatly reducing. Hence, it is very promising for the reuse of retired batteries.

6. Conclusion

This paper proposed a rapid classification method of the retired NCM batteries. As the capacity and internal resistance of retired lithium batteries are quite different, two classification approaches are suggested: the PLF and RBFNN methods. the PLF model is established by the specified tested cells with capacities and their corresponding characteristic voltages. The RBFNN method randomly selects some retired batteries for the model training, and then uses this model to estimate the internal resistance and capacity of the rest retired batteries.

108 cells are used for classification simulation, and 12 cells are subjected to classification experiments. The experimental and simulation results show that the two methods proposed in this paper can be used for accurate estimation of battery capacity and internal resistance, and further used for battery classification. The classification results show a better voltage consistency by the proposed method than random classifications. We further suggest that the PLF and RBFNN methods could be combined for large-scale retired batteries classification. And finally, compared with the traditional method, the proposed methods can greatly reduce the equipment and time cost with satisfactory capacity and internal resistance accuracy.

Declaration of competing interest

The authors declare that they have no known competing financial interests or personal relationships that could have appeared to influence the work reported in this paper.

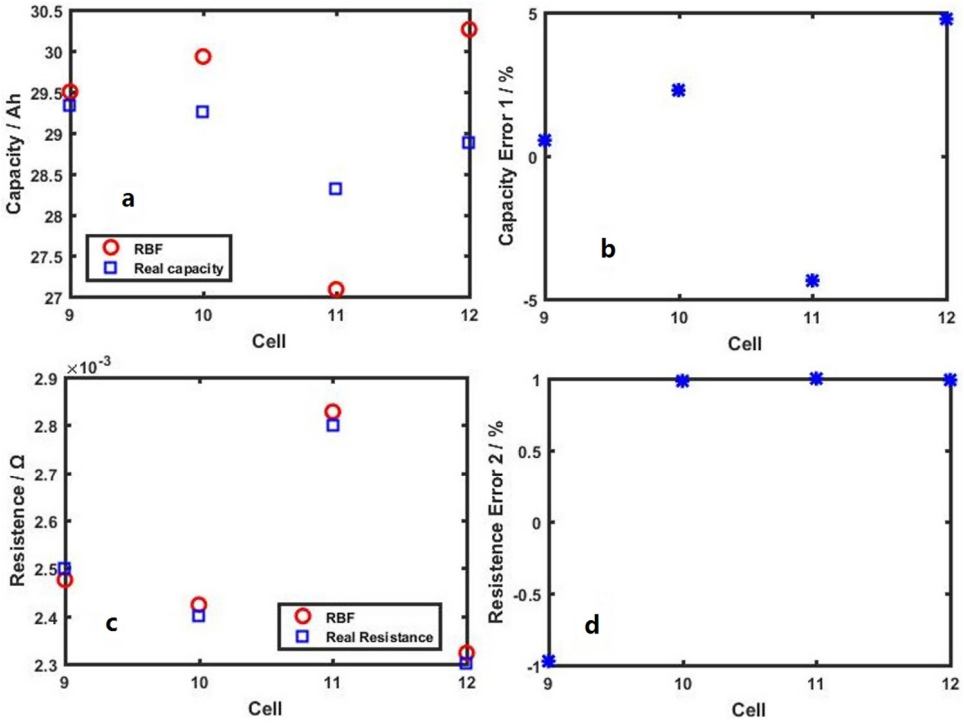

Fig. 12. Estimation results and errors based on the RBFNN method with the experimental data. (a) Capacity estimation; (b) Capacity estimation errors; (c) Resistance estimation; (d) Resistance estimation errors.

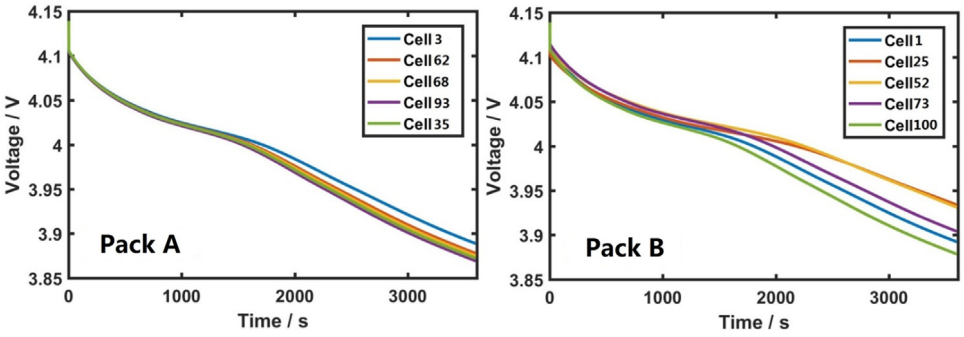

Fig. 13. Discharge curves of Pack A and Pack B.

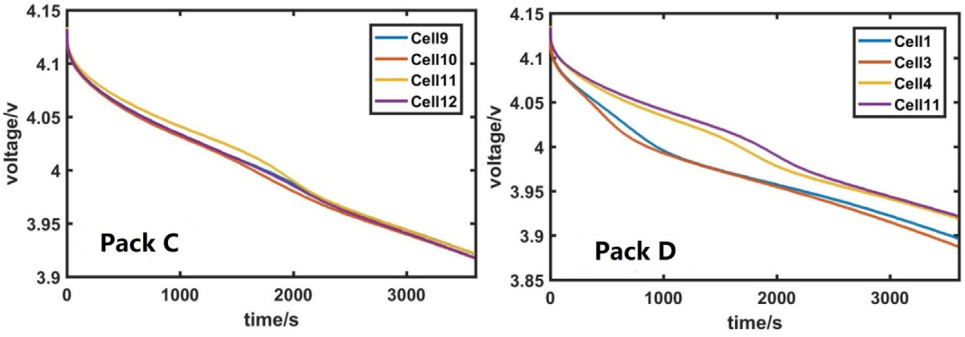

Fig. 14. Discharge curves of Pack C and Pack D.

CRediT authorship contribution statement

Ping Zhou: Methodology, Resources, Supervision, Formal analysis, Writing - review & editing. **Zhonglin He:** Writing - original draft, Software, Data curation, Formal analysis, Writing - review & editing. **Tingting Han:** Funding acquisition, Writing - review & editing. **Xiangjun Li:** Investigation, Visualization. **Xin Lai:** Validation, Formal analysis. **Liqin Yan:** Funding acquisition, Writing - review & editing. **Tiaolin Lv:** Funding acquisition, Writing - review & editing. **Jingying Xie:** Funding acquisition, Writing - review & editing. **Yuejiu Zheng:** Conceptualization, Project administration, Writing - review & editing.

Acknowledgments

This research is supported by the National Natural Science Foundation of China (NSFC) under the Grant number of 51877138, Shanghai Science and Technology Development Fund, PR China 19QA1406200 and the Science and Technology Foundation of State Grid Corporation of China (SGCC) under the contract number of DG71-19-024.

References

Ahmadi, Leila, Fowler, Michael, Young, Steven B., Fraser, Roydon A., Gaffney, Ben, Walker, Sean B., 2014a. Energy efficiency of Li-ion battery packs re-used in stationary power applications. Sustain. Energy Technol. Assess. 8, 9–17. http://dx.doi.org/10.1016/j.seta.2014.06.006.

Ahmadi, Leila, Yip, Arthur, Fowler, Michael, Young, Steven B., Fraser, Roydon A., 2014b. Environmental feasibility of re-use of electric vehicle batteries. Sustain. Energy Technol. Assess. 6, 64–74. http://dx.doi.org/10.1016/j.seta.2014.01.006.

Ambrose, Hanjiro, Gershenson, Dimitry, Gershenson, Alexander, Kammen, Daniel, 2014. Driving rural energy access: a second-life application for electric-vehicle batteries. Environ. Res. Lett. 9 (9), 094004. http://dx.doi.org/10.1088/1748-9326/9/9/094004.

Assunção, André, Moura, Pedro S., de Almeida, Aníbal T., 2016a. Technical and economic assessment of the secondary use of repurposed electric vehicle batteries in the residential sector to support solar energy. Appl. Energy 181, 120–131. http://dx.doi.org/10.1016/j.apenergy.2016.08.056.

Assunção, André, Moura, Pedro S., de Almeida, Aníbal T., 2016b. Technical and economic assessment of the secondary use of repurposed electric vehicle batteries in the residential sector to support solar energy. Appl. Energy 181, 120–131. http://dx.doi.org/10.1016/j.apenergy.2016.08.056.

Barré, Anthony., Deguilhem, Benjamin., Grolleau, Sébastien., Gérard, Mathias., Suard, Frédéric., Riu, Delphine., 2013. A review on lithium-ion battery ageing mechanisms and estimations for automotive applications. J. Power Sources 241, 680–689. http://dx.doi.org/10.1016/j.jpowsour.2013.05.040.

Baumhöfer, Thorsten, Brühl, Manuel, Rothgang, Susanne, Sauer, Dirk Uwe, 2014. Production caused variation in capacity aging trend and correlation to initial cell performance. J. Power Sources 247, 332–338. http://dx.doi.org/10.1016/j.jpowsour.2013.08.108.

Bobba, Silvia, Mathieux, Fabrice, Blengini, Gian Andrea, 2019. How will second-use of batteries affect stocks and flows in the EU? A model for traction Li-ion batteries. Resour. Conserv. Recycl. 145, 279–291. http://dx.doi.org/10.1016/j.resconrec.2019.02.022.

Casals, Lluc Canals, Barbero, Mattia, Corchero, Cristina, 2019. Reused second life batteries for aggregated demand response services. J. Cleaner Prod. 212, 99–108. http://dx.doi.org/10.1016/j.jclepro.2018.12.005.

Dubarry, Matthieu, Liaw, Bor Yann, 2009. Matthieu dubarry bor yann liaw identify capacity fading mechanism in a commercial lifepo4 cell. J. Power Sources 194 (1), 541–549. http://dx.doi.org/10.1016/j.jpowsour.2009.05.036.

Fang, Kaizheng, Chen, Shi, Mu, Daobin, Wu, Borong, Wu, Feng, 2013. Investigation of nickel–metal hydride battery sorting based on charging thermal behavior. J. Power Sources 224, 120–124. http://dx.doi.org/10.1016/j.jpowsour.2012.09.102.

Gaines, Linda, 2014. Linda gaines the future of automotive lithium-ion battery recycling: Charting a sustainable course. Sustain. Mater. Technol. 1–2, 2–7. http://dx.doi.org/10.1016/j.susmat.2014.10.001.

Gur, K., Chatzikyriakou, D., Baschet, C., Salomon, M., 2018. The reuse of electrified vehicle batteries as a means of integrating renewable energy into the european electricity grid: A policy and market analysis. Energy Policy 113, 535–545. http://dx.doi.org/10.1016/j.enpol.2017.11.002.

Heymans, Catherine, Walker, Sean B., Young, Steven B., Fowler, Michael, 2014. Economic analysis of second use electric vehicle batteries for residential energy storage and load-levelling. Energy Policy 71, 22–30. http://dx.doi.org/10.1016/j.enpol.2014.04.016.

Hu, Xiaosong, Feng, Fei, Liu, Kailong, Zhang, Le, Xie, Jiale, Liu, Bo, 2019. State estimation for advanced battery management: Key challenges and future trends. Renew. Sustain. Energy Rev. 114, 109334. http://dx.doi.org/10.1016/j.rser.2019.109334.

Hu, Xiaosong, Xu, Le, Lin, Xianke, Pecht, Michael, 2020. Battery lifetime prognostics. Joule http://dx.doi.org/10.1016/j.joule.2019.11.018.

Hu, Xiaosong, Yuan, Hao, Zou, Changfu, Li, Zhe, Zhang, Lei, 2018. Co-estimation of state of charge and state of health for lithium-ion batteries based on fractional-order Calculus. IEEE Trans. Veh. Technol. 64 (11), 10319–10329. http://dx.doi.org/10.1109/TVT.2018.2865664.

Jiao, Na, Evans, Steve, 2016. Business models for sustainability: The Case of second-life electric vehicle batteries. Procedia CIRP 40, 250–255. http://dx.doi.org/10.1016/j.procir.2016.01.114.

Lai, Xin, Qiao, Dongdong, Zheng, Yuejiu, Ouyang, Minggao, Han, Xuebin, Zhou, Long, 2019. A rapid screecning and regrouping approach based on neural networks for lager-scale retired lithium-ion cells in second-use applications. J. Clean. Prod. 213, 776–791. http://dx.doi.org/10.1016/j.jclepro.2018.12.210.

Lai, Xin, Qiao, Dongdong, Zheng, Yuejiu, Yi, Wei, 2018. A novel screening method based on a partially discharging curve using a genetic algorithm and back-propagation model for the Cascade utilization of retired lithium-ion batteries. Electronics 7 (12), 399. http://dx.doi.org/10.3390/electronics7120399.

Li, Jun, Wang, Yu, Tan, Xiaojun, 2017. Research on the classification method for the secondary uses of retired lithium-ion traction batteries. Energy Procedia 105, 2843–2849. http://dx.doi.org/10.1016/j.egypro.2017.03.625.

Liao, Qiangqiang, Mu, Miaomiao, Zhao, Shuqi, Zhang, Lizhong, Jiang, Tao, Ye, Jilei, Shen, Xiaowang, Zhou, Guoding, 2017. Performance assessment and classification of retired lithium ion battery from electric vehicles for energy storage. Int. J. Hydrog. Energy 42 (30), 18817–18823. http://dx.doi.org/10.1016/j.ijhydene.2017.06.043.

Liu, Chengbao, Tan, Jie, Shi, Heyuan, Wang, Xuelei, 2018. Lithium-ion cell screening with convolutional neural networks based on two-step time-series clustering and hybrid resampling for imbalanced data. IEEE Access 6, 59001–59014. http://dx.doi.org/10.1109/ACCESS.2018.2875514.

Martinez-Laserna, E., Gandiaga, I., Sarasketa-Zabala, E., Badeda, J., Stroe, D.-I., Swierczynski, M., Goikoetxea, A., 2018. Battery second life: Hype, hope or reality? A critical review of the state of the art. Renew. Sustain. Energy Rev. 93, 701–718. http://dx.doi.org/10.1016/j.rser.2018.04.035.

Neubauer, Jeremy, Pesaran, Ahmad, 2011. The ability of battery second use strategies to impact plug-in electric vehicle prices and serve utility energy storage applications. J. Power Sources 196 (23), 10351–10358. http://dx.doi.org/10.1016/j.jpowsour.2011.06.053.

Paul, Sebastian, Diegelmann, Christian, Kabza, Herbert, Tillmetz, Werner, 2013. Analysis of ageing inhomogeneities in lithium-ion battery systems. J. Power Sources 239, 642–650. http://dx.doi.org/10.1016/j.jpowsour.2013.01.068.

Pinsky, N., Gaillac, L., Mendoza, A., Argueta, J., Knipe, T., 2002. Performance of advanced electric vehicle batteries in stationary applications. In: 24th Annual International Telecommunications Energy Conference, Montreal, Quebec, Canada, pp. 366-372. http://dx.doi.org/10.1109/INTLEC.2002.1048682.

Sathre, Roger, Scown, Corinne D., Kavvada, Olga, Hendrickson, Thomas P., 2015. Energy and climate effects of second-life use of electric vehicle batteries in California through 2050. J. Power Sources 288, 82–91. http://dx.doi.org/10.1016/j.jpowsour.2015.04.097.

Saxena, Samveg, Floch, Caroline Le, MacDonald, Jason, Moura, Scott, 2015. Quantifying EV battery end-of-life through analysis of travel needs with vehicle powertrain models. J. Power Sources 282, 265–276. http://dx.doi.org/10.1016/j.jpowsour.2015.01.072.

Schuster, Simon F., Brand, Martin J., Berg, Philipp, Gleissenberger, Markus, Jossen, Andreas, 2015. Lithium-ion cell-to-cell variation during battery electric vehicle operation. J. Power Sources 297, 242–251. http://dx.doi.org/10.1016/j.jpowsour.2015.08.001.

Song, Ziyou, Feng, Shuo, Zhang, Lei, Hu, Zunyan, Hu, Xiaosong, Yao, Rui, 2019. Economy analysis of second-life battery in wind power systems considering battery degradation in dynamic processes: Real case scenarios. Appl. Energy 251, 113411. http://dx.doi.org/10.1016/j.apenergy.2019.113411.

Tian, Jinpeng, Xiong, Rui, Shen, Weixiang, 2019. A review on state of health estimation for lithium ion batteries in photovoltaic systems. eTransportation 2, 100028. http://dx.doi.org/10.1016/j.etran.2019.100028.

Tong, Shi Jie, Same, Adam, Kootstra, Mark A., Park, Jae Wan, 2013. Off-grid photovoltaic vehicle charge using second life lithium batteries: An experimental and numerical investigation. Appl. Energy 104, 740–750. http://dx.doi.org/10.1016/j.apenergy.2012.11.046.

Xu, Xiaolong, Mi, Jifu, Fan, Maosong, Yang, Kai, Wang, Hao, Liu, Jingbing, Yan, Hui, 2019. Study on the performance evaluation and echelon utilization of retired LiFePO4 power battery for smart grid. J. Cleaner Prod. 213, 1080–1086. http://dx.doi.org/10.1016/j.jclepro.2018.12.262.

Zhang, YongZhi, Xiong, Rui, He, HongWen, Qu, Xiaobo, Pecht, Michael, 2019. Aging characteristics-based health diagnosis and remaining useful life prognostics for lithium-ion batteries. eTransportation 1, 100004. http://dx.doi.org/10.1016/j.etran.2019.100004.

Zheng, Yuejiu, Lu, Languang, Han, Xuebin, Li, Jianqiu, Ouyang, Minggao, 2013. LiFePO4 battery pack capacity estimation for electric vehicles based on charging cell voltage curve transformation. J. Power Sources 226, 33–41. http://dx.doi.org/10.1016/j.jpowsour.2012.10.057.

Zheng, Yuejiu, Ouyang, Minggao, Lu, Languang, Li, Jianqiu, 2015. Understanding aging mechanisms in lithium-ion battery packs: From cell capacity loss to pack capacity evolution. J. Power Sources 278, 287–295. http://dx.doi.org/10.1016/j.jpowsour.2014.12.105.

Zheng, Yuejiu, Ouyang, Minggao, Lu, Languang, Li, Jianqiu, Han, Xuebing, Xu, Liangfei, 2014. On-line equalization for lithium-ion battery packs based on charging cell voltages: Part 1. equalization based on remaining charging capacity estimation. J. Power Sources 247, 676–686. http://dx.doi.org/10.1016/j.jpowsour.2013.09.030.

Zheng, Yuejiu, Qin, Chao, Lai, Xin, Han, Xuebing, Xie, Yi, 2019. A novel capacity estimation method for lithium-ion batteries using fusion estimation of charging curve sections and discrete arrhenius aging model. Appl. Energy 251, 113327. http://dx.doi.org/10.1016/j.apenergy.2019.113327.